Functional Materials 11, No.1 (2004)

Collisional dynamics simulation of grafted polymer brushes consisting of anisotropic monomers

I.Neelov[1-3], N.Balabaev[4], M.Ratner[5], F.Sundholm[1], K.Binder[6]

[1]Laboratory of Polymer Chemistry, University of Helsinki,
PB 55, FIN00014, Finland
[2]IRC in Polymer Science and Technology,
University of Leeds, LS2 9JT, Leeds, UK
[3]Institute of Macromolecular Compounds,
31 Bolshoy Pr., 199004 St. Petersburg, Russia
[4]Institute of Mathematical Problems of Biology,
Russian Academy of Sciences, 142292 Pushchino, Russia
[5]Institute for Single Crystals, National Academy of Sciences of Ukraine,
60 Lenin Ave., 61001 Kharkiv, Ukraine
[6]Institute of Physics, J.Gutenberg University,
10 Staudingerweg, D-55099 Mainz, Germany

Received December 7, 2003

We present results of a collisional dynamics simulations of two types of polymer brushes: one containing chains consisting of isotropic monomers ("flexible" brush) and another with large anisotropy of monomers ("anisotropic" brush). Both unperturbed brushes and brushes under shear deformation at constant shear rates were studied. The height of the brush, the elongation and the inclination of the polymer chains in the brush as well as order parameter were calculated at different grafting densities and shear rates. The results are in accordance with available theoretical predictions.

Представлены результаты компьютерного моделирования методом столкновительной динамики двух типов полимерных щёток: первый тип содержит цепочки, состоящие из изотропных мономеров ("гибкая щётка"), тогда как второй тип соответствует сильной анизотропии мономеров ("анизотропная щётка"). Исследованы как невозмущённые щётки, так и щётки под воздействием стационарного сдвигового потока. Длина, высота и наклон щётки, а также параметр порядка вычислены при различных плотностях пришивки. Результаты согласуются с имеющимися теоретическими предсказаниями.

Introduction

Grafted polymer layers consisting of polymer chains terminally anchored at surfaces have many important technological applications [1–3]. Therefore such systems have been studied theoretically since the early 80-ties [4–10] (see also references in reviews [11, 12]) as well as by computer simulation methods. Both Monte Carlo and molecular dynamics methods were applied. Theoretically, experimentally and using computer simulations it was shown that at sufficiently large surface coverage the height of the polymer chains in the direction perpendicular to the surface depends linearly on the polymer length. This regime is usually called the polymer brush regime. Most of computer simulation studies of polymer brushes were devoted to flexible

polymer chains, where the monomers of the chains have a small anisotropy. The dependence of the brush height on grafting density, the density profile and other characteristics of the brushes were obtained by different methods [11–12]. In our research we have used Brownian dynamics (BD) [13–16], self consistent BD [17], stochastic dynamics [18–20] and collisional dynamics (CD) [21] methods. In a recent study the CD method was applied for the first time to investigate flexible polymer brushes consisting of short chains only. In the present work we study the behaviour of longer flexible polymer brushes as well as brushes consisting of anisotropic monomers (anisotropic brushes).

The behaviour of polymer brushes affected by different external forces (compression, stretching, shear) is very important for many practical applications. For example the understanding of the behaviour of polymer brushes under shear deformation is very important for problems such as friction weakening. A theoretical analysis of the behaviour of polymer brushes under the action of tangential forces applied to the ends of grafted chains has been performed on the basis of a scaling approach [22–24] and by analytical SCF theories [25–27]. Since theoretical studies need some simplifying approximations, it is of great interest to study this problem also by computer simulations. Computer simulations of a grafted polymer brush in shear flow were done by Lai and Binder [28] using a non-equilibrium Monte-Carlo method. However the shear flow was introduced rather artificially (by different probabilities of steps in the direction of shear and in the opposite direction). Miao et al [29] used the off-lattice Monte-Carlo method for the analysis of extension and inclination of chains in the brush under shear. However, the shear has been introduced by the same way as by Lai and Binder [28]. Brownian and stochastic dynamics simulation of polymer brushes under shear deformation have been presented by authors earlier [13, 16, 19, 20]. The model and the method were similar to that used in our previous studies [30, 31] for a polymer melt as well as to those of Kremer and Grest [32]. Grest [33] applied the same model for a large-scale molecular dynamics study of the shear force between two brushes consisting of long chains [11]. Theoretical (analytical) approaches to liquid crystalline polymer brushes consisting of polymer chains with anisotropic monomers ("anisotropic brushes") have been described by Birshtein et al [34]. In this paper we report results of collisional dynamics simulations for polymer brushes consisting of polymer chains subjected to shear deformation. Both chains consisting of isotropic and anisotropic monomers were studied. We briefly introduce our model and collisional dynamics method in next part of paper. Description of the process of equilibration of brushes, results of simulations, discussion and concluding remarks are presented in last part.

Description of the Model

Polymer chains were simulated using a bead-rod model, which is composed of N identical mass points (beads) of mass m linked by rigid bonds of length l to a linear chain. Hence, the position vectors r_k, which give the location of the beads with respect to some fixed coordinate system, are subjected to the following constraints

$$(r_{k+1} - r_k)^2 = l^2, \quad k = 1..., N - 1. \qquad (1)$$

In the case of anisotropic brushes each N_c beads ($N_c = 5$ in present paper) along the chain are combined in new rod-like monomer (see Fig. 1) by introducing the additional harmonic potentials between all pairs of beads inside each group of N_c successive beads:

$$U(r_{k+i} - r_k) = K(r_{k+i} - r_k)^2, \qquad (2)$$
$$k = 2, N_c, \; i = 1, N_c - k.$$

If potential is strong enough the average length of the new anisotropic monomer is close to $l' = (N_c-1)*l$. The number of these monomers in a chain is $N' = (N-1)/(N_c-1)$ because each two successive anisotropic monomers have one common bead (see Fig. 1). New anisotropic monomers form freely jointed chain but due to Lennard-Jones interactions of second neighbouring beads (around the bead belonging to both anisotropic monomers) the "valence" angle between new anisotropic monomers can not be smaller than about 60° (the similar limitation of course exists for neighbouring bonds in ordinary linear polymer chains consisting of Lennard-Jones beads.

Contour length of the bead-rod chain is constant and equal to $(N-1)l$ both for flexible and anisotropic brushes. All pairs of mutually nonbonded beads interact through a shifted, short-range repulsive Lennard-Jones potential

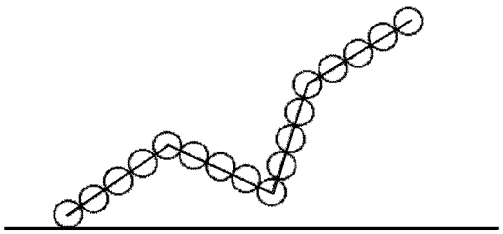

Fig. 1. Fragment of one chain in the brush consisting of 4 anisotropic monomers. Each monomer consists of 5 successive beads on the rod. First bead of first monomer is attached to rigid impenetrable plane.

$$U_R(r) = 4\varepsilon_0[(\sigma/r)^{12} - (\sigma/r)^6] + \varepsilon_0, \quad r \le 2^{1/6}\sigma,$$

$$U_R(r) = 0, \quad r > 2^{1/6}\sigma. \tag{3}$$

Here r is the distance between the beads, and ε_0 is the well depth associated with this potential. In the case of end-grafted chain, we assumed that the grafting surface (wall) is chosen to be the $z = 0$ plane and the first bead of first chain is fixed at one location $\mathbf{r}^1 = (0, 0, 0.5\sigma)$. For the bead-wall interaction, we used the same purely repulsive potential as for the bead-bead interaction, namely, $U_R(z)$, where z is the distance from the bead to the surface. This potential ensures that the beads do not cross the surface and the chain occupies only the space above the surface.

The effective polymer-solvent interaction was simulated by the collisional dynamics [21]. In this method, each bead of the polymer chain suffers collisions with virtual solvent particles. Each stochastic collision is an instantaneous event. Collisions occur in accordance with a Poisson process, which is specified by the only parameter λ, the collisional frequency. Between the stochastic collisions, the system evolves in accordance with the equations of motion as in the usual molecular dynamics. For the bead-rod chain, the equations of motion satisfied by bead i are given by

$$m\frac{d^2 r_i}{dt^2} = -\frac{\partial U}{\partial r_i} + R_i. \tag{4}$$

In the case of the grafted chains, the potential U is composed of two terms corresponding to the bead-bead, U_{bb} and bead-wall, U_{bw}, interactions. The constraint force $\mathbf{R}_i$, acting on bead i is given by

$$R_i = \sum_{j=1}^{N-1} \gamma_j(\delta_{i-1j} - \delta_{ij})(r_{j+1} - r_j), \tag{5}$$

where γ_j, are $N-1$ undetermined Lagrange multipliers associated with the constraints given by Eq.(1), and δ_{ij} is the Kronecker delta. The Lagrange multipliers γ_j are determined by a set of nonlinear equations.

The result of each collision is an instantaneous change in the velocities of the chain beads. Postcollision velocities are found by the solution of the collisional problem. In this problem, the velocity $\boldsymbol{v_0}$ of a virtual solvent particle is chosen at random from the following distribution:

$$P(\mathrm{v}_0 r) = \left(\frac{2\pi k_B T}{m_0}\right)^{-3/2} \exp\left\{-\frac{m_0[\mathrm{v}_0 - w(r)]^2}{2k_B T}\right\}, \tag{6}$$

where T is the solvent temperature, m_0 is mass of the virtual solvent panicle, while $w(r)$ is the hydrodynamic velocity of the solvent at the position $\mathbf{r}$. For steady shear flow in the vicinity of the grafting wall, the flow velocity components were taken as

$$w_x = \dot{\gamma} z, \qquad w_y = w_z = 0, \tag{7}$$

where y is the shear rate, and z is the distance from grafted surface.

Using the collisional dynamics technique described above, we performed simulations of flexible and anisotropic polymer brushes at equilibrium and under shear flow. The polymer brush model consists of M similar polymer chains grafted to a surface $Z = 0$ in a computational cell with periodic boundary conditions in X and Y directions. The first particle of every chain lies on a square lattice in the grafting plane $Z = 0$ (center of particles is at $Z = 0.5\sigma$). The values $M_x = M_y$ are the numbers of grafted chains in the X and Y directions thus total number of chains $M = M_x M_y$. In the present simulation the number of chains $M = 100$ ($M_x = M_y = 10$) and the number N of beads in a chain is 49. For flexible chains the number of chain bonds ("monomers") is $N-1 = 48$. In the case of anisotropic chain each anisotropic monomer in our model consists of $N_c = 5$ beads (geometrical anisotropy of monomer $\varepsilon = 4$) and thus the number of such monomers in chain (consisting of $N = 49$ beads as in flexible chain) is $N' = 12$. We took reduced units in which $m = 1$,

$\sigma = 1$, and $\varepsilon_0 = 1$. We also assumed that rigid bonds are of the length of $l = \sigma$. The equations of motion were integrated using the velocity version of the Verlet algorithm with a time step of 0.005 in reduced units, where the reduced time is given by $t^* = t\sigma^{-1}(m/\varepsilon_0)^{-1/2}$. The mass of virtual solvent molecules was fixed by $m_0 = m$ and a reduced collision frequency per bead was taken as $\lambda^* = \lambda\sigma(m/\varepsilon_0)^{1/2} = 1.3$. The simulations were carried out at a reduced temperature $T^* = k_8T/\varepsilon_0 = 1$ and for a wide range of reduced shear rates $\gamma^* = \gamma\sigma(m/\varepsilon_0)^{1/2}$. We calculated both conformational properties of the polymer chains and the shear viscosity. The viscosity in corresponding reduced units is $\eta^* = \eta\sigma^2(m\varepsilon_0)^{-1/2}$. Further in this work, the reduced units are used exclusively, and for notational simplicity, we drop the * superscript. A more detailed description of the algorithm can be found in ref.[21].

Results and Discussion

Equilibration of the System

In the beginning of each run we equilibrated the system for a long time t_1 from 10^6 to 10^7 integration steps for different values of grafting density and shear rate. We calculated some properties of the chains in the polymer brush (the end-to-end vector and its projections, the end-to-end distance, the average inclination of bonds and the inclination of the chain as a whole with respect to the grafting plane and other quantities) during this time to be sure that equilibration was achieved. The second part of trajectory during time t_2 was used for calculations of mean values, distribution and correlation functions. The value of t_2 was from 10^6 to 10^7 integration steps in different calculations.

Brushes without Shear

The size and the shape of the chains in the brush can be characterized by the mean square end-to-end distance $<h^2>$ and its components: $<h_x^2>$, $<h_y^2>$ and $<h_z^2>$ (the mean square projections on the grafting plane (x and y projections) and height of the brush (z projection), correspondingly).

Another quantitative characteristic of the chain's size and shape are the mean square radius of gyration $<R_g^2>$ and its projections $<R_{gx}^2>$, $<R_{gy}^2>$ and $<R_{gz}^2>$. It is well known [6, 11, 12] that in good solvents at big enough values of the grafting density s (corresponding to significant overlapping of grafted chains) the height of the brush $h_z = (<h_z^2>)^{1/2}$ and the value of $R_{gz} = (<R_{gz}^2>)^{1/2}$ must be proportional to the number N of monomers in the chain, anisotropy of segment ε as $\varepsilon^{1/3}$ and grow with the grafting density s as $s^{1/3}$. Thus, due to excluded volume interactions the chains in the brush are partially stretched in the direction perpendicular to the grafting surface.

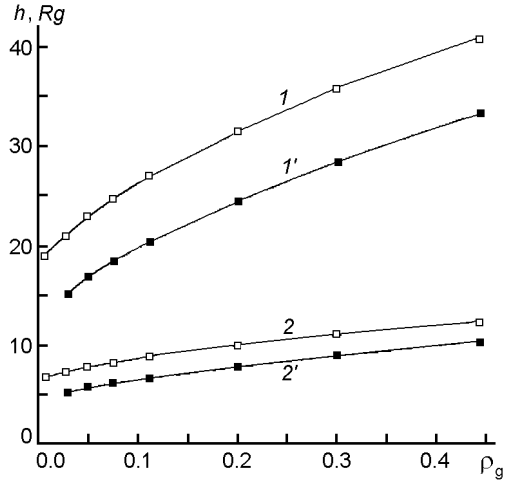

Fig. 2. The mean square end-to-end distance h of the chain *1*, *1′* and radius of gyration R_g *2*, *2′* vs grafting density; $N = 49$, $M = 100$. The curves *1* and *2* are for anisotropic and curves *1′* and *2′* for flexible brushes.

With no shear applied the z projection of the chain size give the main contribution to the total chain size. The dependences of the mean square end-to-end distance $h = (<h^2>)^{1/2}$ and radius of gyration $R_g = (<R_g^2>)^{1/2}$ calculated in the present work are plotted in Fig. 2 and characteristics of the brush height h_z and R_{gz} are shown on Fig. 3. From these plots an d from Table 1 one can see that both the total size and the height of brushes consisting of anisotropic monomers are near 1.6 times larger than the corresponding values for normal brushes in all cases. The theoretical evaluation [6] gives for our brushes with anisotropy $\varepsilon = 4$ the ratio of brush heights $\varepsilon^{1/3} = 1.6$ which is close to values 1.3–1.4 obtained in simulation (see Table 1). Value obtained in simulation can be a little bit less because the anisotropic monomers in our model actually not quite rigid but have some small flexibility. At the same time the qualitative behaviour of these characteristics as function of grafting density s is similar for both types of brushes (see Fig. 2 and Fig. 3). We obtained that in the brush

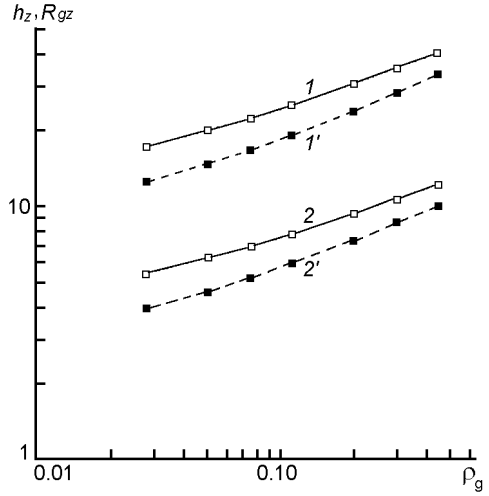

Fig. 3. The mean thickness of the brush: *1*, *1′* — the *z* component h_z of the end-to-end vector, *2*, *2′* — the *z* component R_{gz} of the square of the radius of gyration of the chain vs grafting density; *1*, *2* for anisotropic and *1′*, *2′* for flexible brushes.

regime the slope of dependence of R_{gz} on s (Fig. 3) (in double logarithmic scale) for anisotropic brushes is equal to 0.34. For ordinary brushes of the same contour length it is about 0.32. Thus, both these values are close to the theoretical value of 1/3 for flexible polymer brushes. There was no systematic difference between the brushes with respect to the dependence on grafting density when no shear was applied for both types of brushes.

Orientational ordering of monomers in the direction perpendicular to grafting surface was compared for both brushes. It was shown that ordering for anisotropic brushes is higher at all grafting densities. Order parameter S_2 increased gradually (see Table 1) with grafting density for both type of brushes in accordance with results of Chen and Fwu.

Brushes under Shear

We studied the influence of shear flow on the behaviour of both types of polymer brushes at the high grafting density $s = 0.44$. The mean square end-to-end distance of chains in brush and their mean square gyration radius were calculated (Fig. 4) as well as height of brush, *Z*-component of gyration radius and average height of monomers above plane (Fig. 5). Inclination of chains relatively plane (Fig. 6) and intrinsic viscosity (Fig. 7) were obtained also. The results show that at small shear rates up to $g = 0.001$ both anisotropic and flexible

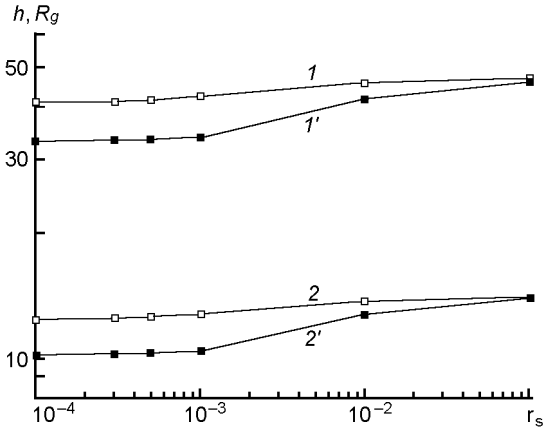

Fig. 4. The mean square end-to-end distance *h* of the chain *1*, *1′* and radius of gyration R_g *2*, *2′* vs shear rate; $N = 49$, $M = 100$. *1*,*2* for anisotropic and *1′*, *2′* for flexible brush.

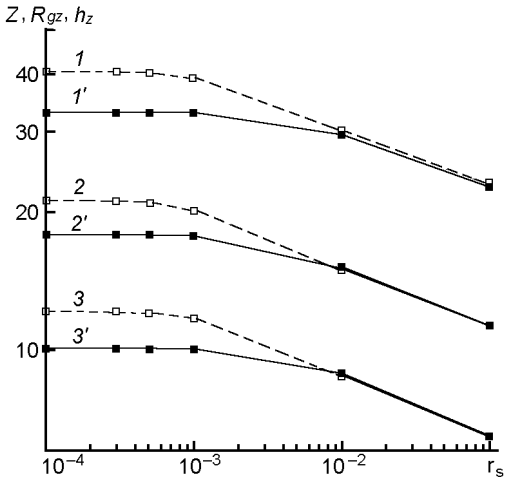

Fig. 5. The mean thickness of the brush: *1*, *1′* — *z* component of the square of the end-to-end vector; *2*, *2′* — *z* component of the square of the radius of gyration of the chain; *3*, *3′* — average *z*-coordinate of the chains beads vs shear rate. *1*, *2*, *3* for anisotropic and *1′*, *2′*, *3′* for flexible brush.

brushes are not influenced by shear flow (see Fig. 4, Fig. 5 and Fig. 7). Both dimensions and shear viscosity were practically constant in this interval of *g*. At larger shear rates *g* the total size of the chains in a brush (h and R_g) increases (Fig. 4). Shear force causes additional stretching and inclination of chains in the direction of shear. At the same time the brush height h_z (and related value R_{gz}) begin to decrease (Fig. 5). Similar picture we observed earlier employing Brownian and stochastic dynamics as well as collisional dynamics for shorter

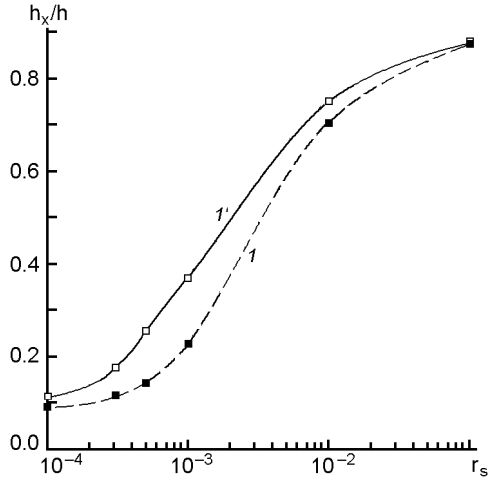

Fig. 6. The inclination of a chain as a function of the shear rate: *1* — for anisotropic brushes, *1′* — for flexible brushes.

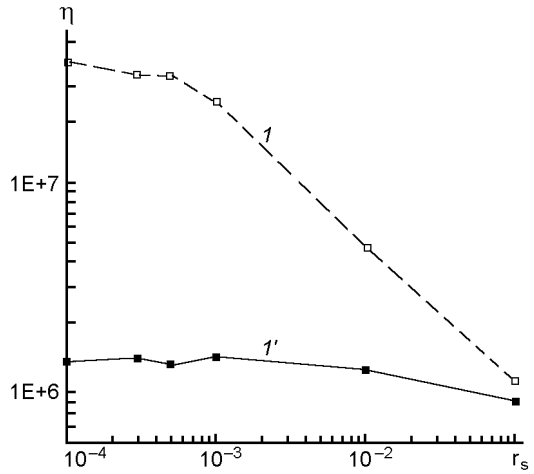

Fig. 7. Intrinsic viscosity as function of shear rate: *1* — for anisotropic brushes, *1′* — for flexible brushes.

Table 1.

	Grafting density							
	0.007	0.025	0.050	0.075	0.100	0.200	0.300	0.400
Ratio of brushes heights	1.38	1.38	1.37	1.34	1.31	1.28	1.25	1.18
Order parameter								
Flexible brush	0.01	0.03	0.04	0.06	0.08	0.15	0.23	0.37
Anisotropic brush	0.05	0.09	0.12	0.16	0.20	0.36	0.51	0.71

Table 2.

	Shear rate				
	0	0.0003	0.001	0.01	0.1
Cosine of inclination angle					
Flexible brush	0	0.06	0.21	0.72	0.88
Anisotropic brush	0	0.15	0.37	0.75	0.88
Order parameter					
Flexible brush	0.37	0.37	0.38	0.67	0.89
Anisotropic brush	0.71	0.72	0.77	0.93	0.97

flexible chains. For anisotropic brushes studied in this paper this decrease begin at smaller values of shear rate $g = 0.001$ than for flexible brushes where it occurs near $g = 0.01$.

The inclination of the brushes (Fig. 6 and Table 2) begins to increase at weak shear even before the total dimension h and brush height h_z start to respond to the shear flow. It means that at low shear deformation the inclination of the main axis of the chains (Fig. 6) in the brush may occur mainly due to an increase in the x-component of the dimension of the chains without any variation in the z-component (in the brush thickness). This type of behaviour of the brush under weak shear has been predicted by Rabin and Alexander [37]. At stronger deformation the effect of finite extensibility appears and any further inclination of the grafted chains must be accompanied by a decrease in the brush thickness. At very large shear rates when the chains tend to completely extended conformation these dependences flatten out. At

large extensions the h_x component gives the main contribution to the total chain size h. The decrease of the third component of the chain size h_y with shear is faster than for the brush height h_z. This can be understood with the aid of simple arguments. Stretching of the chains in the x-direction results in re-partitioning of steps of the corresponding random walk so that the fraction of steps in the direction h_y perpendicular to the chain axis decreases.

However, a decrease in the number of steps in the z-direction results in a decrease in the brush height and, consequently, in an increase of the repulsive interaction between monomers of stretched chains that is unfavourable. Thus the chain increases the number of steps in the x direction mostly due to a decrease of number of steps in the y-direction while the number of steps in the z-direction decrease more slowly. Due to this fact and due to smaller initial (no shear) values of the y component in comparison with the z component the final values of h_y are very small. The order parameter increase gradually with shear rate for both brushes (see Table 2) but at all shear rates its value is greater for brush consisting of anisotropic monomers. The direction of this orientation changes from direction perpendicular to plane in the absence of flow to direction almost parallel to plane at high shear rates.

Dependence of the intrinsic viscosity η on shear rate is presented on Fig. 7. One can see that at small shear rates the value of η for anisotropic brushes is essentially higher than for ordinary flexible brushes. In the case of flexible brushes the value of η is nearly constant until shear rate near 0.001 while for anisotropic brushes the value of η slightly decreases already at lesser shear. At higher shear rates there is stronger decrease of η with shear (especially for anisotropic brushes) and at extremely high shear rates (near 0.1) the viscosity of both brushes become close to each other. These behaviour is correlate with changes in conformation and orientation of chains (Fig. 4–6) and is in agreement with our previous Brownian dynamics simulation results for flexible brushes in shear flow at different grafting densities. The equal viscosity of flexible and anisotropic brushes at large shear rates was expected because at this conditions chain in both brushes have near the same structure: they are near completely extended and and inclined relatively grafting plane (see Fig. 4–6).

Conclusions

Results of collisional dynamics simulations of two types of polymer brushes are presented. We studied both unperturbed brushes at different grafting densities and brushes under shear flow. Both conformational properties of the chains in the brush and intrinsic viscosity have been calculated.

The results show that the height of the brush as a function of grafting density s follows the same power law $s^{1/3}$ in both cases. The brushes consisting of anisotropic monomers are more extended at the same contour length of the chain. The ratio of brush heights (for anisotropic and isotropic brushes) is in agreement with theory of Birshtein and Zhulina for semiflexible brushes. It was found that the intrinsic viscosity η for anisotropic brushes is essentially higher than for isotropic brushes at small shear rates but this difference decreases with shear.

Two stages were obtained in the deformation for both types of the brushes with increasing shear:

i) Increase of the x component h_x of the end-to-end distance without decrease of brush height h_z (at shear rates $g<g_c$)

ii) Additional increase of h_x due to the decrease of h_z.

This behaviour is in agreement both with theoretical predictions and with our previous BD simulation of ordinary flexible brushes.

The onset of the brush deformation gets displaced to larger shear rates as the density of grafting increases. In our model this characteristic value of the shear rate depends on the number of monomers in the chains as well. However, if hydrodynamic interactions were taken into account the penetration of the solvent flow into the brush would be much smaller. The characteristic penetration length will be independent on N. Hence the characteristic value of the shear rate corresponding to the onset of the brush deformation in realistic system is expected to be virtually independent on N.

Our next goal is to study more anisotropic brushes and incorporate the hydrodynamic interactions into the present model.

Acknowledgement. The authors are grateful to the European Science Foundation (SUPERNET Program), The Academy of Finland and INTAS (grant No.99-1114 and 00-712) for financial support and CSC for computer time on IBMSC parallel computer.

References

1. D.Napper, Polymer Stabilization of Colloidal Dispersions, Academic Press, London (1983).
2. S.Wu, Polymer Interfaces and Adhesion, Dekker, NY (1979).
3. J.Klein, D.Perahia, S.Warburg, *Nature*, **352**, 143 (1991).
4. S.Alexander, *J. Phys.*, **38**, 983 (1977).
5. P.G.De Gennes, *Macromolecules*, **13**, 1069 (1980); *Adv. Colloid and Interface Sci.*, **27**, 189 (1988).
6. T.Birshtein, E.Zhulina, *Polymer. Sci.*, **25**, 2165 (1983); *Polymer*, **25**, 1453 (1984).
7. T.Birshtein, A.Mercurieva, V.Pryamitsyn, A.Polotsky, *Macromol. Theory & Simul.*, **5**, 215 (1996).
8. V.Amoskov, T.Birshtein, V.Pryamitsyn, *Macromolecules*, **29**, 7240 (1996).
9. T.Birshtein, V.Amoskov, A.Mercurieva, V.Pryamitsyn, *Macromol. Theory & Simul.*, **113**, 115 (1997).
10. T.Birshtein, A.Mercurieva, L.Klushin, A.Polotsky, *Comput. Theor. Polymer Sci.*, **8**, 179 (1998).
11. G.Grest, *Adv. Polym. Phys.*, **138**, 149 (1999).
12. T.Birshtein, V.Amoskov, *Polymer. Sci.*, **C42**, 172 (2000).
13. I.Neelov, K.Binder, in: Proc. of the Conf. Molecular Mobility and Order in Polymer Systems, St.Petersburg, p.23 (1994).
14. I.Neelov, K.Binder, *Macromol. Chem., Theory & Simul.*, **4**, 119 (1995).
15. I.Neelov, K.Binder, *Macromol. Chem., Theory & Simul.*, **4**, 1063 (1995).
16. I.Neelov, K.Binder, *Polymer. Sci.*, **A38**, 665 (1996).
17. M.Saphiannikova, I.Neelov, V.Pryamitsyn et al., *Rheol. Acta*, **39**, 469 (2000).
18. I.Neelov, F.Sundholm, K.Binder, *J. Non-Cryst. Solid*, **235–237**, 731 (1998).
19. I.Neelov, O.Borisov, K.Binder, *Macromol. Chem., Theory & Simul.*, **7**, 141 (1998).
20. I.Neelov, O.Borisov, K.Binder, *J. Chem. Phys.*, **108**, 6973 (1998).
21. N.Balabaev, A.Lemak, L.Lunevskaya et al., *Mechanics of Composite Materials and Constructions*, **5**, 16 (1999).
22. Y.Rabin, S.Alexander, *Europhys. Lett.*, **13**, 49 (1990).
23. J.L.Barrat, *Macromolecules*, **24**, 3704 (1991).
24. T.Birshtein, E.Zhulina, *Macromol. Chem., Theory & Simul.*, **1**, 193 (1992).
25. E.Zhulina, A.Halperin, *Macromolecues*, **25**, 5730 (1992).
26. A.Johner, J.-F.Joanny, *J. Chem. Phys.*, **96**, 6257 (1992).
27. J.-F.Joanny, *Langmuir*, **8**, 989 (1992).
28. P.Y.Lai, K.Binder, *J. Chem. Phys.*, **98**, 2366 (1993).
29. L.Miao, H.Guo, M.J.Zuckermann, *Macromolecules*, **29**, 2289 (1996).
30. Yu.Gotlib, N.Balabaev, A.Darinskii, I.Neelov, *Macromolecules*, **13**, 602 (1980).
31. A.Darinskii, I.Neelov, Preprint SCBI Acad. Sci. USSR, Pushchino (1981) [in Russian].
32. G.S.Grest, K.Kremer, *Phys. Rev. A*, **33**, 3628 (1986).
33. G.S.Grest, *Phys. Rev. Lett.*, **76**, 4979 (1996).
34. T.Birshtein, V.Amoskov, *Comput. Theor. Polym. Sci.*, **10**, 159 (2000).
35. A.Lemak, N.Balabaev, *J. Comput. Chem.*, **17**, 1685 (1996).
36. A.Lemak, N.Balabaev, Y.Karnet, Y.Yanovsky, *J. Chem. Phys.*, **108**, 797 (1998).
37. Y.Rabin, S.Alexander, *Europhys. Lett.*, **3**, 49 (1990).

Моделювання полімерних щіток, які містять анізотропні мономери методом динаміки зіткнень

І.Неєлов, М.Балабаєв, М.Ратнер, Ф.Сандхолм, К.Біндер

Наведено результати комп'ютерного моделювання методом динаміки зіткнень двох типів полімерних щіток: перший тип містить ланцюжки ізотропних мономерів ("гнучка щітка"), тоді як другий тип відповідає анізотропії мономерів ("анізотропна щітка"). Досліджено як незбурені щітки, так і щітки під впливом стаціонарного зсувного потоку. Довжина, висота та нахил щітки, а також параметр порядку обчислені при різних щільностях пришивки. Результати збігаються з теоретичними завбаченнями, що маються.